

Fracture behavior and biocompatibility evaluation of nylon-infiltrated porous hydroxyapatite

A. NAKAHIRA, M. TAMAI, S. MIKI, G. PEZZOTTI

Department of Chemistry and Materials Technology, Kyoto Institute of Technology,
Gosho-kaido-cho, Matsugasaki, Sakyo-ku, Kyoto 606-8585, Japan

E-mail: nakahira@ipc.kit.ac.jp

Hybrid hydroxyapatite/polymer composites were prepared by the infiltration of nylon into porous hydroxyapatite. Porous hydroxyapatite (HAp) bodies were prepared from a whisker-like powder with high aspect ratio by pressureless-sintering at various temperatures. Pore characteristics, such as the fraction of open porosity and the pore size distribution, were designed and evaluated by mercury porosimeter. Through the *in situ* polymerization of ϵ -caprolactam, infiltrated into the porous HAp body, a polymeric secondary phase network interpenetrated with the HAp phase was obtained. The obtained hybrid HAp/nylon composites were evaluated with respect to their fracture behavior, i.e., fracture energy, and *in vitro* bioactivity in simulated body fluid (SBF) in the present paper. These HAp/nylon hybrid composite have a K_{IC} of 1.65 MPam^{1/2} and also a good bioactivity according to the results of SBF immersion tests.

© 2002 Kluwer Academic Publishers

1. Introduction

Hydroxyapatite (HAp) is a useful bioceramic, because of its superior biocompatibility as well as bioglass and AW-glass [1]. For bone and teeth repairs, biomaterials are demanded of both good biocompatibility and reliable mechanical properties for long periods. However, the nature of the HAp bonding results in low fracture toughness and fracture energy, similar of those of glasses [2]. According to other authors, the fracture toughness and fracture energy of monolithic HAp are reported to be approximately 0.7–1.0 MPam^{1/2} and 1.0 J/m², respectively [3]. The disadvantage of such poor intrinsic properties makes difficult clinical and orthopedic applications. Therefore, while the improvement of the fracture properties by the addition of a secondary phase is necessary for actual applications, at the same time, to maintain the biocompatibility characteristics of HAp is a mandatory requirement. For example, when the incorporation of tetragonal ZrO₂ to a HAp matrix was attempted to improve the fracture toughness through a transformation toughening mechanism, the diffusion of calcium due to decomposition of HAp into tricalcium phosphate led to full stabilization of the ZrO₂ particles after the sintering process [4, 5]. Also, it was reported that the hot-pressed Al₂O₃-platelet toughened HAp composites had a toughness of 2.0 MPam^{1/2} [6]. However, a drastic improvement of the fracture energy of HAp by the dispersion of a ceramic phase is difficult, because of the low intrinsic fracture toughness and fracture energy of ceramic phases. Furthermore, coating of HAp onto metals or Al₂O₃ implants also have been tried, but the coated layer is also affected by brittleness [7, 8].

A different approach for the achievement of improved fracture energy and toughness characteristics is to use an infiltration technique. Infiltration of molten metals, polymers, and ceramics into porous ceramics through various processings is a potentially successful technique [9–11]. Especially, polymer infiltration into porous hydroxyapatite would be advantageous to fabricate high-performance composites, because of the variety of polymers available and their good mechanical properties. The obtainment of high-performance HAp-polymer hybrid composites much demands on the control of the HAp matrix microstructure. In particular, a well-designed pore structure, pore size and pore distribution is imperative [12, 13]. In this paper, the design of the porosity characteristics of HAp is first pursued, and then the hybridization of such a porous body with nylon as a basic study is attempted to prepare a new biomaterial composite for bone replacement.

In our experiments, we attempted to control the porous structure by using a starting whisker-like HAp powder with high aspect ratio. It was possible to fabricate a porous HAp body with a high open porosity fraction and a well-percolated pore distribution upon sintering. A 6-nylon polymer was selected for the hybridization of the porous structure, because of its good mechanical properties and good inertness in the human body.

2. Experimental procedure

Whisker-like hydroxyapatite powder was synthesized through the hydrolysis of tricalcium phosphate in a mixture of the binary system of H₂O and isopropyl

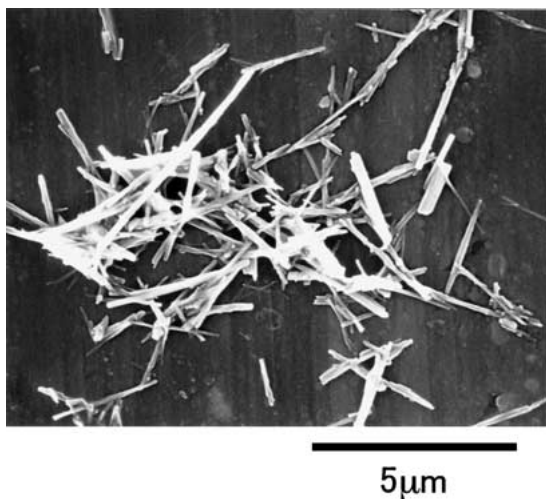


Figure 1 SEM micrograph of the whisker-like hydroxyapatite.

alcohol [14]. Fig. 1 shows a scanning electron microscopy (SEM) micrograph of the whisker-like hydroxyapatite powder. The average length and diameter of the whisker-like hydroxyapatite were 2–5 μm and 0.1 μm , respectively, corresponding to an aspect ratio ≈ 20 –30. Porous hydroxyapatite bodies were prepared from this whisker-like HAp.

By first uniaxially pressing the powder, disks with 15 mm in diameter and 5 mm in thickness compacted with a stainless steel die under 5 MPa were obtained. The compacts of HAp were then again pressed by a cold isostatic pressing under 50 MPa. These green compacts were sintered by pressureless sintering method in the temperature interval between 800 and 1000°C, with a heating rate of 5 K/min. Sintered porous HAp bodies were cut with a diamond blade. The cut surfaces were ground by a diamond wheel and polished with diamond paste. Phase identification was carried out by X-ray diffraction analysis. The density was measured by the Archimedes' method. The porosity characteristics, pore-size distribution average and median pore-size values, were evaluated with a mercury porosimeter (Autopore III, Micrometrics). Microstructure of sintered hydroxyapatite bodies was observed with an SEM (S-800, Hitachi).

Porous sintered hydroxyapatite bodies were set in a vacuum furnace and infiltrated with ϵ -caprolactam by capillary action. As an initiator 6-aminohexanoic acid was used for *in situ* polymerization to 6-nylon upon heating at 200°C for 18 h. The polymerization process to form 6-nylon was fast and deeply spreading into the porous HAp body. After *in situ* polymerization, the samples were ground with an abrasive paper in order to remove the extra nylon from their surfaces. Finally, HAp/nylon hybrid samples were cut with a diamond blade and polished with diamond paste.

Young's modulus of HAp/nylon hybrid composites was evaluated according to the flexural vibration method [15]. The dimension of HAp/nylon hybrid composites used for mechanical testing was $2 \times 3 \times 30$ mm. Fracture energy was measured according to the single-edge double notched beam (SEDNB) method [16]. The span of the three-point bending test geometry was 20 mm. The notch was cut with a diamond wheel with

a 0.5 mm thickness. Additional sharpening of the notch root was obtained with a thin stainless blazer [17]. The microstructure of hybrid composites and fractured surfaces of samples after fracture tests were observed with an SEM. The bioactivity of these HAp/nylon hybrid composites were evaluated by *in vitro* test in the simulated body fluid (abbreviated to SBF) developed by Kokubo *et al.* [18]. This SBF had the ion concentrations nearly equal to the human body plasma, which were prepared by dissolving reagent-grade, NaHCO_3 , NaCl , KCl , CaCl_2 , Na_2SO_4 , $\text{K}_2\text{HPO}_4 \cdot 3\text{H}_2\text{O}$, $\text{MgCl} \cdot 3\text{H}_2\text{O}$ into ion-exchanged and distilled water and buffered at pH 7.25 with tris(hydroxymethyl)aminomethane and HCl at 36.5°C.

3. Results and discussion

3.1. Microstructure and properties of porous HAp bodies

Fig. 2 shows the variation of relative density with sintering temperature for the whisker-like HAp powder. The pore fraction of green compacts obtained from the whisker-like powder was approximately 65%. The sintered bodies from the whisker-like HAp powder exhibited a relative density as low as 35% at 800–900°C and 40% at 1000°C, respectively. A relative density almost independent from sintering temperature is a peculiar characteristic of the whisker-like powder, while the density of samples sintered from spherical HAp powder drastically increased with sintering temperature [19]. A fraction of open porosity almost independent of densification temperature plays an important role in designing the mechanical properties of both porous skeleton and hybrid composites, as discussed afterward.

Fig. 3 shows the pore size distribution of HAp bodies sintered from whisker-like powder at 800, 900, and 1000°C. The samples sintered at 800 and 900°C showed no closed pores and their open porosities were approximately 100%. In case of the sample sintered at 1000°C, the volume fraction of open pores was about 95%. As reported elsewhere [20], samples sintered at 900°C from spherical HAp powder showed 50% of

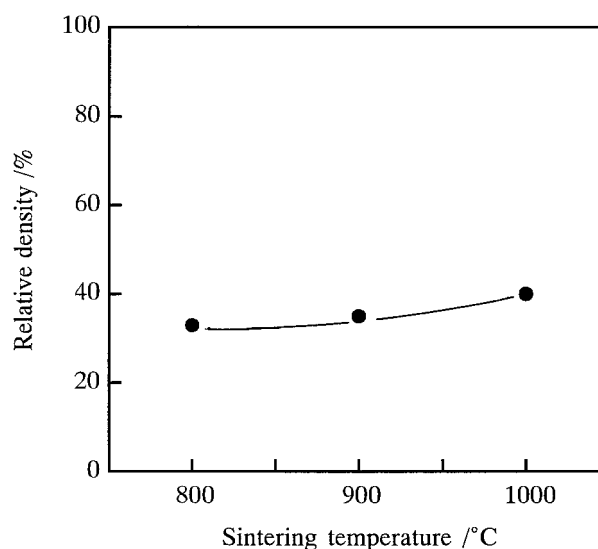


Figure 2 Variation of relative density with the sintering temperature for whisker-like hydroxyapatite.

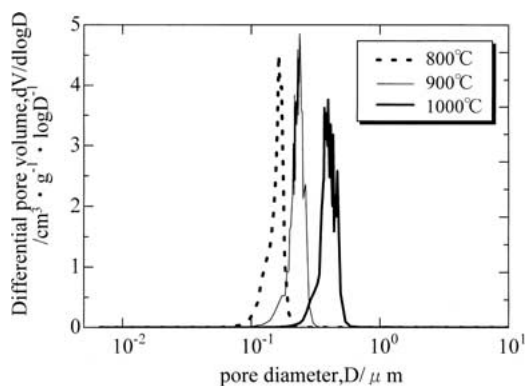


Figure 3 Pore volume and pore size distribution of hydroxyapatite sintered at 800, 900, and 1000°C.

relative density and 70% of open porosity fraction. As seen in Fig. 3, all samples showed a sharp distribution of pore size, mainly below 1 μm . Samples sintered at 800°C showed pores with average diameter of 0.2 μm . In the case of samples prepared at 900°C the pore diameter was in the range of 0.2–0.3 μm . At 1000°C, the pore diameter varied from 0.5 to 0.8 μm . During sintering no pore was eliminated, therefore, no densification occurred in the temperature interval between 800 and

900°C. The HAp body prepared at 1000°C, especially possesses a very sharp pore size distribution, varying from 0.5 to 0.8 μm .

Fig. 4a and b show SEM photographs of samples sintered at 800 and 900°C, respectively. Sintering at 800–900°C produced a fine whisker-like structure with no grain growth occurred during sintering. On the contrary, pressureless-sintering at 1000°C produced some grain growth and the development of thick whisker, (cf. Fig. 4c). Large open-pores were still observed in the HAp skeletons prepared at $\geq 900^\circ\text{C}$. These results suggest that using a raw whisker-like HAp powder results in an extremely porous microstructure, in which approximately 100% of the pores were open.

The distribution of open-pore diameter (i.e., the maximum of volume distribution function), and the relative density are plotted in Fig. 5. The pore diameter increased with sintering temperature. It was reported that the pore diameter was almost nanometer-sized in samples from spherical HAp raw powder and increased with pressureless-sintering temperature [19, 20]. Pressureless sintering compacts from whisker-like HAp powder is a very effective method for achieving open pores and, thus for fabricating a highly fibrous skeleton structure.

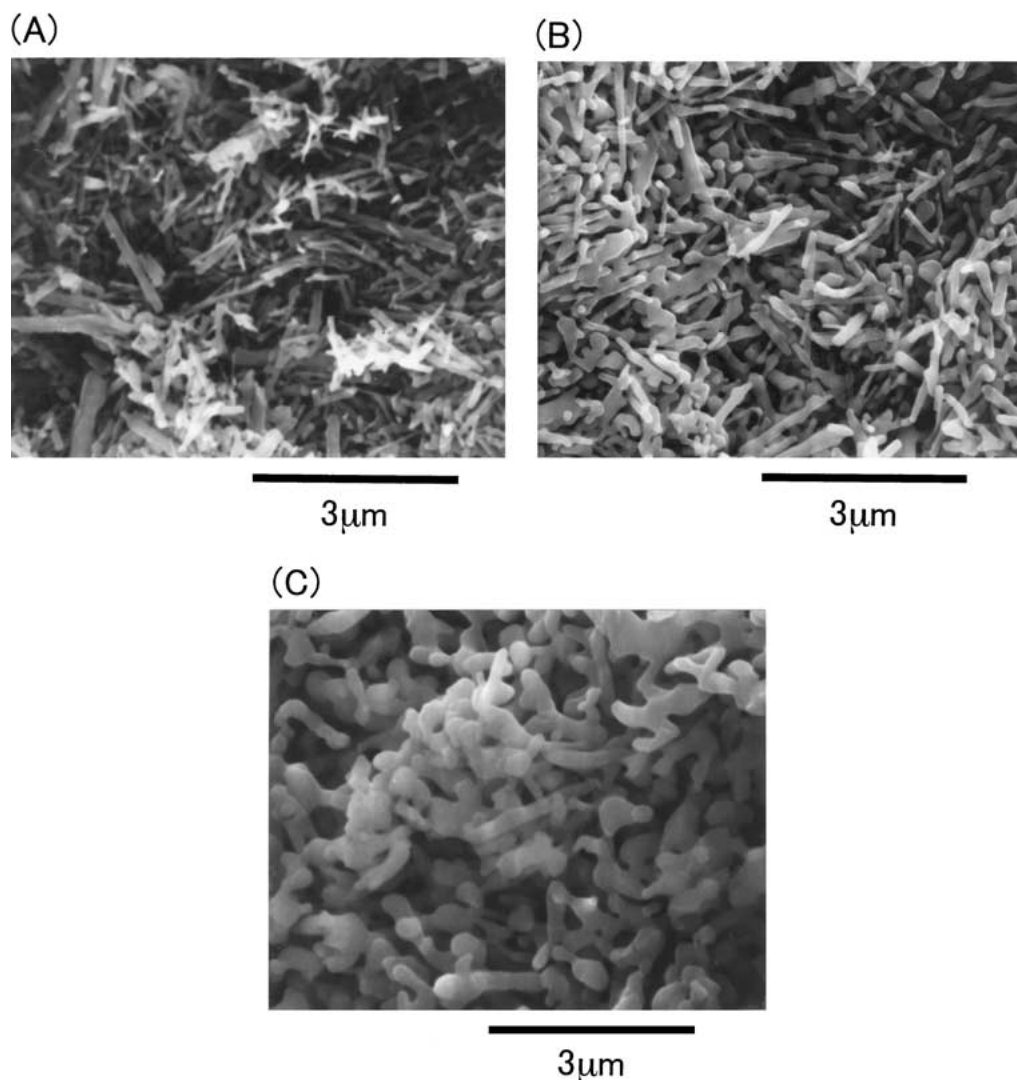


Figure 4 SEM micrographs of whisker-like hydroxyapatite sintered at various temperatures. (A) 800°C, (B) 900°C, (C) 1000°C.

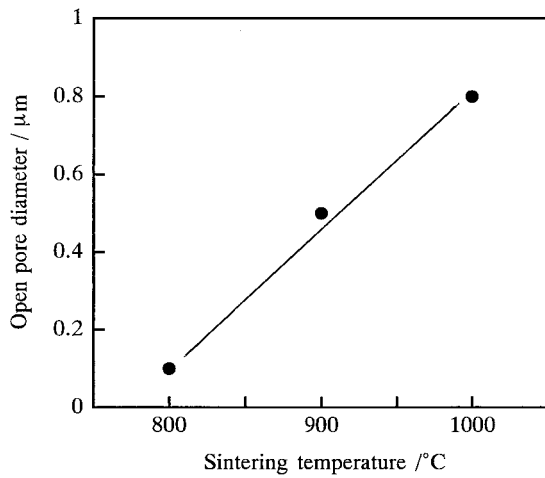


Figure 5 Relationship of open pore diameters and relative density of whisker-like hydroxyapatite sintered at 800, 900, and 1000°C.

3.2. Hydroxyapatite/nylon hybrid composites and their properties

Infiltration of ϵ -caprolactam, as a nylon monomer, into the highly porous HAp specimens sintered at 800 to 1000°C, and successive *in situ* polymerization were attempted. Fig. 6 shows an SEM micrograph of the internal microstructure of a hybrid nylon-infiltrated hydroxyapatite composite. SEM observation of the hybrid nylon-infiltrated HAp composites revealed that 6-nylon polymer was homogeneously dispersed into the porous skeleton, although some residual pores were also observed. Using density data as shown in Table I, approximately 10% of porosity was confirmed for the composites after hybridization. This result coincided with

TABLE I Some properties of hybrid nylon-infiltrated hydroxyapatite composites from porous HAp samples with 54% of porosity

	Density (%)	Young's modulus (GPa)	Fracture energy (J/m ²)
Hybrid nylon-infiltrated HAp composites	90.3	51.2	20.8

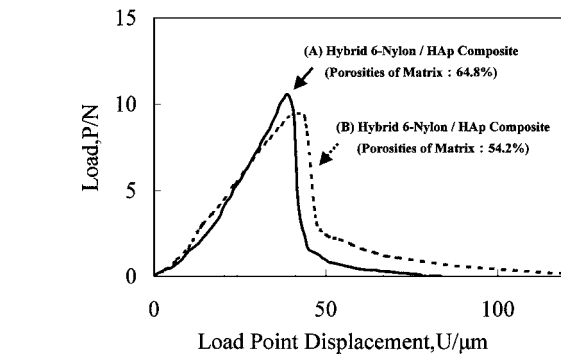
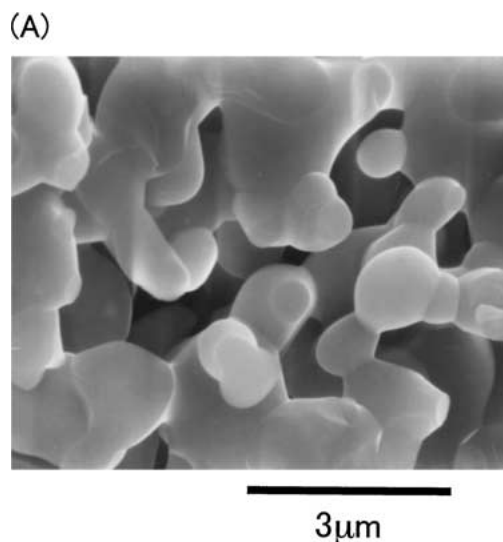


Figure 7 Diagram of load and load point displacement for hybrid nylon-infiltrated hydroxyapatite composites. (A) 800°C, (B) 1000°C.

the presence of pores occasionally observed by SEM. Fig. 7 shows the diagram of load and load point displacement for hybrid nylon-infiltrated hydroxyapatite composites. Both hybrid nylon-infiltrated hydroxyapatite composites prepared from porous hydroxyapatite samples with 65% and 54% of porosity showed stable fracture behavior. The area under load-displacement curve was computed and divided by twice the fracture surface area measured by SEM observation in order to evaluate the value of work of fracture (WOF). Fracture energy, fracture toughness and Young's modulus of hybrid nylon-infiltrated hydroxyapatite composites from porous samples with 54% of porosity are summarized in Table I. Hybrid nylon-infiltrated hydroxyapatite composites exhibited a fracture energy of approximately 21 J/m², whereas the fracture energy of natural bone was reported to be 1–2 J/m² [21]. The value of WOF for the HAp/nylon hybrid composites was significantly high, similar to that measured in earlier studies for bovine femur [22]. The existence of residual pores in the hybrid nylon-infiltrated hydroxyapatite composite may inhibit the furthermore increase of fracture energy and fracture toughness. This hybrid composite from porous hydroxyapatite samples with 54% of porosity showed the stable fracture behavior and resulted in a rising R-curve behavior with crack extension, as shown in Fig. 8. The value of K_{10} for the HAp/nylon hybrid

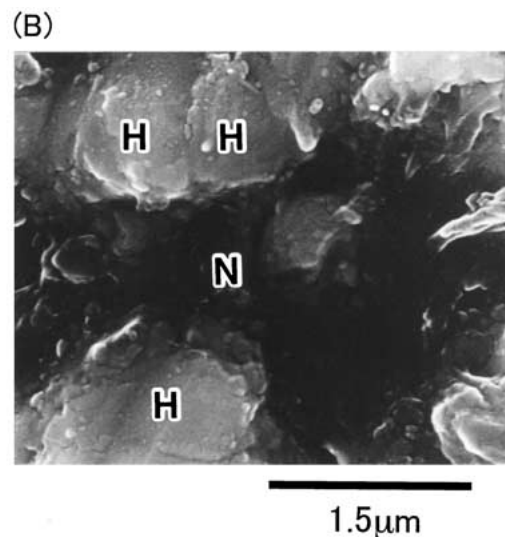


Figure 6 SEM micrographs of the microstructure of porous hydroxyapatite bodies sintered at 800°C (A) and the internal microstructure of hybrid nylon-infiltrated hydroxyapatite composites after infiltration and polymerization of ϵ -caprolactam as a nylon monomer (B). H = HAp, N = 6-nylon.

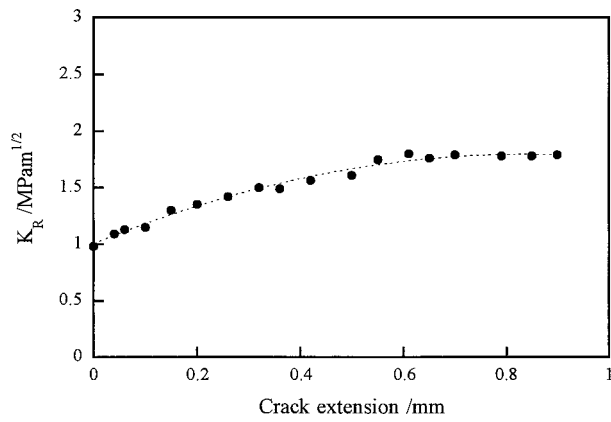


Figure 8 R-curve behavior of hybrid nylon-infiltrated hydroxyapatite composites.

composite ($K_{I0} = 0.9 \text{ MPam}^{1/2}$) was twice that of monolithic HAp ($K_{I0} = 0.4 \text{ MPam}^{1/2}$), which reached a value of $1.65 \text{ MPam}^{1/2}$ after a crack extension of approximately $700 \mu\text{m}$.

Fig. 9A shows a SEM image of crack profile for a hybrid nylon-infiltrated hydroxyapatite composite. A crack-bridging mechanism due to nylon polymer was observed by SEM. Therefore, the increase in fracture energy of hybrid nylon-infiltrated hydroxyapatite composites was achieved by the bridging effect and plastic deformation owing to stretching of nylon polymer ligaments along the crack wake.

Fig. 10 shows the results after *in vitro* immersion in SBF solution at 36.5°C for 1 day and 14 days. Fine bone-like hydroxyapatite did not form on the surface

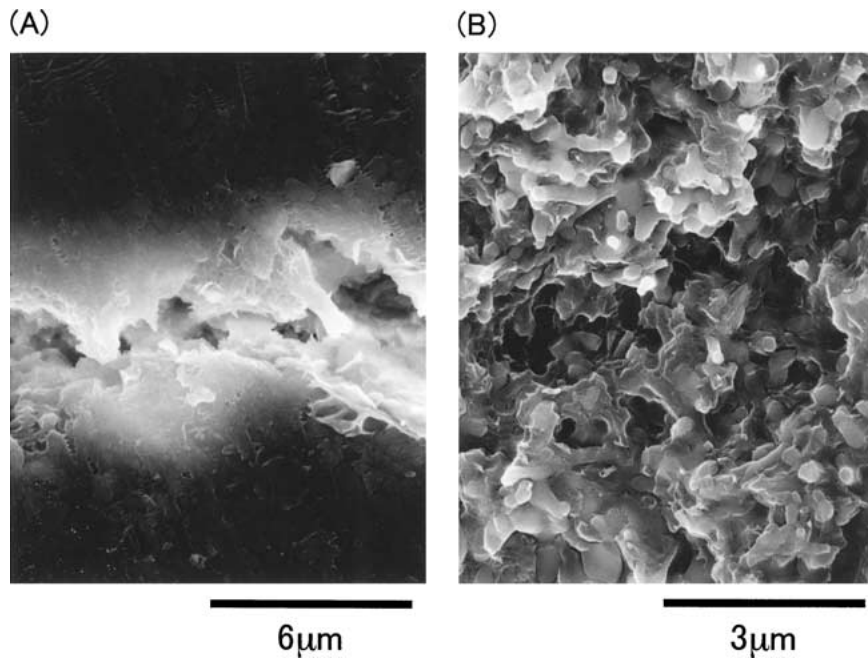


Figure 9 SEM observation of crack propagation for hybrid nylon-infiltrated hydroxyapatite composites. (A) crack propagation (B) fracture surface.

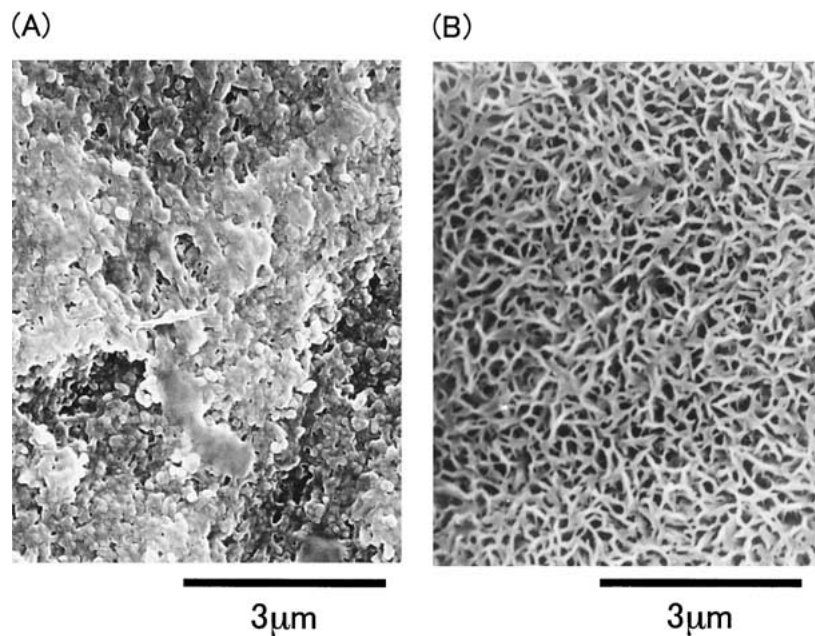


Figure 10 *In vitro* results after the immersion in 1.0 SBF solution at 36.5°C for 1 day (A) and 14 days (B).

of nylon-infiltrated HAp composites after 1 day. However, SEM observation after 14 days showed that the surface of nylon-infiltrated hydroxyapatite composites was coated with a thick bone-like layer. This layer homogeneously covered the whole surface of the composite and consisted of a sponge-like structure, according to observation performed at higher magnification. From the results in SBF, it is concluded that the nylon-infiltrated HAp composites possess a good bioactivity.

4. Conclusion

Porous HAp bodies were prepared from a whisker-like raw powder with high aspect ratio by pressureless-sintering at various temperatures. Samples sintered from whisker-like powder exhibited an open fraction of porosity of approximately 100% at 800–900°C and 95% even at 1000°C. The pore size gradually increased with sintering temperature. A narrower pore size distribution and the presence of large pores with an average diameter of 0.5–0.8 μm were found after pressureless-sintering at 1000°C. SEM observation showed a skeleton-structure of HAp with well-grown necking between grains, which implies a strong bonding between the acicular grain. Using whisker-like HAp as a starting powder resulted in extremely porous microstructures, namely a highly fibrous skeleton structure, independent of sintering temperature.

Infiltration of a polymeric secondary phase into such HAp porous bodies with well-developed penetrated pores led to the formation of a homogeneous hybrid nylon-infiltrated HAp composite. The hybrid nylon-infiltrated HAp composite sintered at 1000°C exhibited a rising R-curve behavior with crack extension and a high fracture energy value of approximately 21 J/m². The increase in fracture energy of hybrid nylon-infiltrated hydroxyapatite composites was achieved by a crack bridging mechanism with plastic deformation of nylon ligaments. According to *in vitro*

results of SBF test, the nylon-infiltrated HAp composites possessed an excellent bioactivity.

References

1. L. L. HENCH, *J. Amer. Ceram. Soc.* **74** (1994) 1487.
2. R. I. MARTIN and P. W. BROWN, *J. Mater. Sci.: Mater. Med.* **6** (1995) 138.
3. K. A. HING, S. M. BEST and W. BONFIELD, *ibid.* **10** (1999) 135.
4. J.-M. WU and T. S. YEY, *J. Mater. Sci.* **23** (1988) 3771.
5. N. TAMARI, M. MOURI and I. KONDO, *Yogyo-kyokai-shi* **95** (1987) 806.
6. S. GAUTIER, E. CHAMPION and D. BERNACHE-ASSOLLANT, *J. Mater. Sci.: Mater. Med.* **10** (1999) 533.
7. T. BRENDEL, A. ENGEL and C. RUSSEL, *ibid.* **3** (1992) 175.
8. C.-J. LIAO, F.-H. LIN, K.-S. CHEN and J.-S. SUN, *Biomaterials* **20** (1999) 1807.
9. D. COUPARD, J. GONI and J. F. SYLVAIN, *J. Mater. Sci.* **34** (1999) 5307.
10. C. TOY and W. D. SCOTT, *J. Amer. Ceram. Soc.* **73** (1993) 97.
11. R. D. VELTRI and F. S. GALASSO, *ibid.* **73** (1990) 2123.
12. K. A. HING, S. M. BEST and W. BONFIELD, *J. Mater. Sci.: Mater. Med.* **6** (1995) 138.
13. M. NANKO and K. ISHIZAKI, *Phys. Rev. B* **56** (1997) 6968.
14. A. NAKAHIRA, K. SAKAMOTO, S. YAMAGUCHI, M. KANENO, S. TAKEDA and M. OKAZAKI, *J. Amer. Ceram. Soc.* **82** (1999) 2029.
15. M. SHIMADA, K. MATSUSHITA, S. KURATANI and T. OKAMOTO, *ibid.* **67** (1984) 23.
16. G. PEZZOTTI, O. SBAIZERO, V. SERGO, N. MURAKI, K. MARUYAMA and T. NISHIDA, *ibid.* **81** (1998) 187.
17. T. NISHIDA, Y. HANAKI, T. NOJIMA and G. PEZZOTTI, *ibid.* **77** (1995) 606.
18. T. KOKUBO, H. KUSHITANI, S. SAKKA, T. KITSUGI and T. YAMAMURO, *J. Biomed. Mater. Res.* **24** (1990) 721.
19. A. NAKAHIRA, M. TAMAI, K. SAKAMOTO and S. YAMAGUCHI, *J. Ceram. Soc. Jpn.* **108** (2000) 99.
20. M. TAMAI, S. MIKI, G. PEZZOTTI and A. NAKAHURA, *ibid.* **108** (2000) 915.
21. L. L. HENCH and J. WILSON, in "An Introduction to Bioceramics" (World Scientific Publishing, Singapore, 1993) p. 1.
22. G. PEZZOTTI, S. N. F. ASMS, L. P. FERRONI and S. MIKI, *J. Nat. Sci. Nat. Ned.*, in press.

Received 17 October 2001

and accepted 2 July 2002